Bone 120 (2019) 9–19

Contents lists available at ScienceDirect

Bone

journal homepage: www.elsevier.com/locate/bone

Full Length Article

Alendronate improves bone density and type I collagen accumulation but increases the amount of pentosidine in the healing dental alveolus of ovariectomized rabbits

Nilo Guliberto Martins Chavarry[a], Daniel Perrone[b], Maria Lucia Fleiuss Farias[c], Bernardo Camargo dos Santos[d], Andrea Castro Domingos[e], Alberto Schanaider[f], Eduardo Jorge Feres-Filho[a,*]

[a] Division of Graduate Periodontics, School of Dentistry, Federal University of Rio de Janeiro, RJ CEP 21941-971, Brazil
[b] Laboratory of Nutritional Biochemistry and Food, Chemistry Institute, Federal University of Rio de Janeiro, RJ CEP 21941-909, Brazil
[c] Division of Endocrinology, School of Medicine, Federal University of Rio de Janeiro, RJ CEP 21941-913, Brazil
[d] Department of Nuclear Engineering (COPPE), School of Engineering, Federal University of Rio de Janeiro, RJ CEP 21941-972, Brazil
[e] Department of Oral Pathology, Oral Radiology and Oral Diagnosis, School of Dentistry, Federal University of Rio de Janeiro, RJ CEP 21941-971, Brazil
[f] Department of Surgery, School of Medicine, Federal University of Rio de Janeiro, RJ CEP 21941-913, Brazil

ARTICLE INFO

Keywords:
Osteoporosis
Bisphosphonate
Type I collagen
Pentosidine
Rabbits
HPLC

ABSTRACT

Background: It has been shown that the oral aminobisphosphonate sodium alendronate (ALN) therapy reduces the risk of main fractures in osteoporotic women, but its effect on the jaw bones is poorly known. Here, we hypothesized that ALN affects the newly formed alveolar bone, particularly the quality of the type I collagen cross-linking.

Methods: Osteoporosis was induced by ovariectomy (OVX) in 6-month old rabbits. Six weeks following surgery, eight animals were treated by oral gavage with ALN (OVX + ALN) and ten received placebo (OVX + Pbo). Another six rabbits which were sham operated also received placebo (SHAM + Pbo). One month following the beginning of treatment, the upper and lower left first premolars were removed. Six weeks later, the upper and the lower right first premolars were also extracted. One month after the second extraction, biopsies were collected from the maxillary extraction sites and collagen crosslinks were analyzed in the newly formed bone tissue by HPLC. Also, at this time, mandibular bone segments were subjected to μCT.

Results: Animals treated with ALN achieved a roughly 2-time greater bone volume fraction value at a late healing period than animals in the other groups ($p < 0.05$). Collagen mean results were 2- to 4-times superior in the OVX + ALN group than in the control groups ($p < 0.05$).

ALN-treated animals presented higher amounts of the non-enzymatic collagen cross-link pentosidine (PEN) than the sham-operated rabbits ($p < 0.05$), whereas the OVX + Pbo group presented the highest amount of PEN ($p < 0.05$).

Conclusion: Alendronate increases bone volume and collagen accumulation, but does not fully rescue the non-osteoporotic alveolar tissue quality as is evident from the increased quantity of pentosidine.

1. Introduction

Osteoporosis is a progressive skeletal disorder characterized by reduction of bone mineral density (BMD) and degeneration of bone microarchitecture [1]. That results in bone fragility and fracture, which adversely impact the quality of life and boost the risk of infection and mortality [2]. Estrogen deficiency due to menopause is the main cause of bone loss in women and bisphosphonates (BPs) are the most commonly prescribed class of drugs for its treatment by suppressing bone resorption [3]. These pharmacological agents can reduce the risk of fractures and the rate of mortality related to hip fracture by up to 30% and 60%, respectively [4,5]. Clinical studies in postmenopausal women showed that long-term use of those drugs resulted in persistent anti-fracture and BMD increasing effects beyond three years of treatment [6]. However, in the last decade there have been reports of a greater than before incidence of atypical femur fractures (AFFs)

* Corresponding author.
E-mail address: eduardoferes@odonto.ufrj.br (E.J. Feres-Filho).

https://doi.org/10.1016/j.bone.2018.09.022
Received 22 April 2018; Received in revised form 23 September 2018; Accepted 24 September 2018
Available online 30 September 2018

associated with long-term BPs therapy, which might be explained by an impaired bone remodeling [7,8]. The continuing and degrading action of BPs on the skeleton fracture-resistance toughening system has indeed been associated with bone fragility [9,10].

Nitrogen-containing BPs accumulate mainly in areas of high osteogenic activity, such as sites of micro fracture repair and dental alveolus healing [11,12]. This might result in local amplification of BP effects, leading to modifications in the organic matrix molecular features and bone mineralization [13,14]. Molecular alterations in the extracellular matrix may interfere with the mineralization process and lead to a brittle osseous tissue. In fact, a higher material modulus (less compliant bone), which might contribute to tissue embrittlement and fracture risk enhancement, was correlated with accumulation of the non-enzymatic glycation-induced pentosidine in a mouse model of type 2 diabetes [15]. That form of advanced glycation end product (AGE), contrasting to the enzyme lysyl oxidase-derived collagen cross-links, has been proposed as a major cause of bone fragility associated with aging and numerous disease states including osteoporosis [16]. Due to its exceptionally high proportion of approximately 90% of the organic matter, it is generally agreed that collagen plays a critical role in the structure and function of bone tissue [17]. Here, we hypothesized that the anti-resorptive therapy with sodium alendronate, an aminobisphosphonate, would affect the type I collagen cross-linking pattern and the quality of the newly-formed alveolar bone after tooth extraction.

2. Materials and methods

This study was approved by the Ethics Committee for the Use of Animals by the Health Sciences Center of the Federal University of Rio de Janeiro (UFRJ, protocol number 007/15), according to the regulations in effect in Brazil. This scientific paper complies with the EU Directive 2010/63 for animal experiments and it is also in agreement with the National Institutes of Health Guide for the Care and Use of Laboratory Animals (NIH Publications No. 8023, revised 1978) and follows the ARRIVE guidelines.

2.1. Animal model

Twenty eight, 6-month old, New Zealand white rabbits (*Oryctolagus cuniculus*), skeletally mature, and weighing approximately 4 kg were randomly distributed into the following experimental groups: Sham-operation + placebo (SHAM + Pbo, $n = 8$); Ovariectomy + placebo (OVX + Pbo, $n = 10$); Ovariectomy + alendronate (OVX + ALN, $n = 10$). The identified animals were housed in individual cages at the laboratory animal facility/Experimental Surgery Center of the School of Medicine at the UFRJ and maintained in controlled environment conditions (20 to 25 °C, 30% to 35% humidity and a 12 h light/12 h darkness cycle). Animals were fed a balanced rabbit chow and water ad libitum.

2.2. Bone mineral density

Animals had the whole-body BMD measured by dual-energy x-ray absorptiometry (DXA, Lunar Prodigy Advance Plus, GE Lunar, Milwaukee, WI, USA) at three different time points: baseline, six weeks after ovariectomy and 12 weeks following the beginning of medication/placebo administration. Exams were carried out under general anesthesia by IM administration of xylazine 5 $mg \cdot kg^{-1}$ and ketamine 35 $mg \cdot kg^{-1}$, in duplicate, by the same trained examiner who was blinded to the experimental group allocation. Images were captured in the standard scanning mode of 1.8 μGy with the Lunar Prodigy Advance software (GE Healthcare, Chicago, IL, USA) specific for small animals.

2.3. Surgical procedures

One week after the baseline bone densitometry, bilateral ovariectomy was carried out under general anesthesia with xylazine and ketamine. The animals were intubated, and anesthesia was maintained with isoflurane 1.5% and oxygen 0.8–1.5 $L \cdot min^{-1}$, using a non-rebreathing circuit. The surgical procedure was performed as follows: after a longitudinal incision in the lower third of the abdomen, both distal uterine horns were ligated followed by ovaries removal. The abdominal cavity was closed by muscle and skin layers suture. In addition, animals received the antibiotic enrofloxacin 2.5 $mg \cdot kg^{-1}$ (Baytril 10%, Bayer, São Paulo, Brazil) and the anti-inflammatory/analgesic ketoprofen 1.0 $mg \cdot kg^{-1}$ (Ketojet 100 mg, AgenerUnião, Apucarana, PR, Brazil) medication, both given IM once daily for five days. One week following the surgery, ovariectomized animals were fed low calcium (0.14%) and phosphorus (< 1%) diet (Algomix Agroindustrial Ltda, Ouro Verde do Oeste, PR, Brazil) for six weeks according to an established osteoporosis model for rabbits [18]. Sham-operated animals received a regular diet. After that six week period, animals started receiving either ALN or placebo according to the experimental group allocation.

2.4. Interspecies extrapolation of drug dose and dosing interval

The dose conversion of ALN 70 mg once-weekly [19] from a 70 kg human to a 4 kg rabbit was based on the metabolic size, measured by the minimum energy cost (MEC), and the metabolic rate, measured by the specific minimum energy cost per unit weight (SMEC), according to the equations: $MEC = K.W_{kg}^{0.75}$, and $SMEC = K.W_{kg}^{0.75}/W_{kg}$, respectively. In those equations, "K" means a theoretical constant of proportionality that, in line with the Hainsworth's energy group to which placental mammals belongs, equals to 70; "W_{kg}" is the weight of the animal species; and the exponent "0.75" refers to the slope of the metabolic regression line [20]. Firstly, the MEC dose was calculated by using the equation: MEC dose = treatment dose in humans / MEC in humans; the treatment dose in rabbits was, then, computed by using the equation: treatment dose in rabbits = MEC dose x MEC in rabbits. After the calculation, one ended up with a dose of ALN 2.03 $mg \cdot kg^{-1}$. Secondly, the dosing interval was determined from the SMEC. To accomplish that, one has to calculate the following equation: SMEC interval in humans = SMEC in humans × dosing interval in humans. Afterwards, to estimate the treatment interval in rabbits, the SMEC interval in humans was divided by the SMEC in rabbits. The result was an 82.14 h interval. To avoid overstressing the animals, it was established an adjusted drug regimen of 16 mg dissolved in distilled water to a final volume of 16 mL, administered by oral gavage once weekly for twelve weeks. Placebo groups received 16 mL of distilled water. The oral gavage procedure was executed under gas sedation (isoflurane 1.5% and oxygen 0.8–1.5 $L \cdot min^{-1}$), using a flexible cannula attached to a syringe.

2.5. Tooth extraction

One month following the beginning of drug/placebo treatment, the upper and the lower left first premolars were removed for late healing analyses. Six weeks later, the upper and the lower right first premolars were extracted for early healing studies. Tooth extraction was carried out under general anesthesia with xylazine and ketamine. Access to the extraction site was facilitated by an external approach, which consisted of 1 cm extension incision from the labial commissure to the last molar, as previously described [21]. Mucoperiosteal flap was raised to expose the tooth cervical area and the surrounded alveolar bone. Periotome and pediatric dental forceps were used for tooth luxation and extraction, respectively. Tissue wound was closed in two layers with absorbable polyglycolic acid 4-0 suture and skin was closed with nylon 4-0 suture. One month after the second extraction procedure, animals were sacrificed with a 100 $mg \cdot kg^{-1}$ thiopental sodium intracardiac injection, under general anesthesia.

2.6. Sample collection

Immediately after euthanasia, jaw bones were dissected out and cleaned off of any soft tissue. Subsequently, they were snap frozen and kept in liquid nitrogen until the time of analysis by spectrophotometry and high-performance liquid chromatography (HPLC) or stored in buffered formaldehyde 10% (v/v), aqueous solution (formalin), until being firstly subjected to μCT and next to CBCT. Maxillary cylindrical samples from areas relative to the right and left first premolars alveoli were collected with a 4.3 mm/10.0 mm trephine bur. Mandibular segments encompassing the edentulous areas and measuring 3 cm from the mental foramen to the third molar were removed with a double-faced diamond disc.

2.7. Newly-formed bone microstructure

Each mandibular bone sample was scanned and reconstructed into a digitized 3D image using a μCT Skyscan 1173 (Bruker Co., Kontich, Belgium), with a voxel size of 14.96 μm. The X-ray tube was operated at 55 kV with a current of 145 μA and a 1.0 mm width aluminum filter. Five radiographic projections were obtained changing the y-axis randomly at 0.40° step interval with samples rotation of 360°. The mean scanning time was 40 min per sample.

Two-dimension image projections were archived in 16 bit-TIFF and used for cross-sectional image reconstruction with a NRecon 1.6.5.8 software (Bruker Co.), based on a 3D connectivity measurement algorithm [22]. From the stored bitmap images, using CTAn (CT Analyser V. 1.14.4.1 - Bruker Co.), a circular region of interest (ROI) with 4 mm diameter was set on the alveolar bone between the first and last slice using the "interpolate" tool for the intermediary slices. The total cylindrical volume of interest (VOI, Fig. 1) was checked to cover just the tooth extraction area, starting at the first axial strip above the mandibular canal and finishing at 4 mm from the initial, totaling 269 slices. The newly-formed bone VOI was segmented using a gray-value automatic threshold according to Otsu's method. For the quantitative analysis of the trabecular bone microstructure, at 4 or 10 weeks after tooth extraction, the following structural parameters were determined: bone volume fraction (BV/TV [%]), trabecular pattern factor (Tb.Pf [1/mm]), structure model index (SMI), trabecular number (Tb.N [1/mm]), trabecular thickness (Tb.Th [mm]), trabecular separation (Tb.Sp [mm]), connectivity density (Conn.D [$1/\mu m^3$]), bone surface density (BS/TV [1/mm]) and degree of anisotropy (DA). Analyses were carried out by the same trained examiner without information regarding the experimental group allocation.

Fig. 1. Representative image of the total cylindrical volume of interest (VOI), encompassing the apical/mid-section of the tooth extraction area.

2.8. Newly-formed bone fractal analysis by CBCT

The same mandibular samples which were analyzed by μCT were afterward examined by cone beam computed tomography (CBCT). Fractal dimensions of each image were calculated by the box counting technique [23]. Images were obtained with a PreXion 3D scanner, reconstructed with a PreXion 3D software (PreXion Inc., San Mateo, CA), and stored as JPG. A region of interest (ROI) relative to the apical portion of the healing alveolus just above the mandibular canal was selected with the ImageJ 1.47v software (NIH, Bethesda, MD). Next, the ROIs were duplicated and blurred by a 35 pixel-Gaussian filter. The blurred image was subtracted from the original image and a gray value of 128 was added to the result at each pixel location. This process allowed each image to have a uniform density. The resultant image was binarised and segmented into components representing the trabeculae in white and bone marrow space in black. The image was, then, inverted to make the trabeculae black. Subsequently, the image was eroded and dilated to minimize noise and, lastly, skeletonized. Analyses were executed in duplicate by a single trained examiner who was blinded to the experimental group allocation.

2.9. Quantification of type I collagen and collagen cross-links

Type I collagen analysis was performed according to the methodology described elsewhere [24], with minor modifications. Frozen maxillary cylindrical samples, measuring 3.6 mm (diameter) × 8 mm (length), were ground to a powder in a metal grinder. Approximately 20 mg of ground bone were hydrolyzed in 2 mL 6 M HCl at 110 °C for 20 h in sealed glass tubes. The amount of collagen was calculated based on the assumption that 1 mol of collagen contains 300 nanomoles of hydroxyproline which content was determined by spectrophotometry in the hydrolyzed bone extracts with a commercial kit following the manufacturer's specifications (Sigma-Aldrich, St. Louis, MO, USA).

Mature type I collagen cross-links pyridinoline, deoxypyridinoline (respectively PYD, DPD - Quidel Corporation, San Diego, CA) and pentosidine (PEN - Cayman Chemical, Ann Arbor, MI) were analyzed by HPLC in a Shimadzu system (Shimadzu Corp., Kyoto, Japan), containing a LC-20AT quaternary pump, a CBM-20A controller, a DGU-20A5R degassing unit and a RF-10AXL fluorescence detector. Before being injected, samples were concentrated under N_2 flow and added to an internal standard solution (INT STD; Quidel Corporation, San Diego, CA). Cross-links were separated in an Atlantis dC18 reverse phase column (3 μm, 4.6 mm × 100 mm), protected by a guard column (both from Waters Corp., Milford, MA, USA). Mobile phase flow rate was 1.2 mL·min^{-1}. Gradient elution was comprised by solvent A (12% aqueous solution of Heptafluorobutyric Anhydride [HFBA; Sigma-Aldrich, St Louis, MO]) and solvent B (50% of solvent A and 50% acetonitrile). PYD, DPD and INT STD fluorescence was monitored in 297 nm and 395 nm excitation and emission wave lengths, respectively. For detection of PEN, excitation and emission wavelengths were altered to 335 and 385 nm, respectively. Cross-links were identified by retention time and quantified by peak area internal standardization, utilizing intern standard to compensate for possible loss of analytes during sample preparation. All analyses were performed in duplicate without any information of the experimental identity of the sample.

2.10. Statistical analysis

Statistical analyses were carried out with the Statistical Package for the Social Science, version 21 (SPSS, Chicago, IL). Experimental data were subjected to the Kolmogorov-Smirnov test and verified to be normally distributed. Hence, mean results of bone mineral density across experimental groups (OVX + ALN, OVX + Pbo, SHAM + Pbo) at different time points throughout the study (baseline, 6 weeks post-OVX/SHAM surgery and 12 weeks of ALN/Pbo medication), mean results of new alveolar bone microstructure parameters, and collagen and cross-link contents in the experimental groups at the early and late healing stages were compared by one-way ANOVA, followed by Bonferroni *post-hoc* test. Differences were considered statistically significant at $p < 0.05$.

3. Results

Four animals were lost at various moments of this study. The remaining rabbits (OVX + ALN, $n = 8$; OVX + Pbo, $n = 10$; SHAM + Pbo, $n = 6$) did not present any macroscopic signal of infection.

3.1. Bone mineral density

At baseline, there was no statistically significant difference in mean BMD values among experimental groups. In contrast, approximately 6 weeks following surgery, ovariectomized rabbits exhibited a statistically significant 22.5% lower mean BMD than sham-operated animals. At the same time point, the ovariectomized animals presented a statistically significant 17% mean BMD reduction from baseline. At the final examination, animals in the OVX + ALN group demonstrated a BMD return to baseline levels and a statistically significant 12.7% higher mean BMD compared to the OVX + Pbo group (Fig. 2). *Post-hoc* calculation indicated that the intergroup comparison, throughout time, on this parameter (primary variable) was powered at 95%.

3.2. Newly-formed alveolar bone morphometry and microstructure features

All groups presented comparable newly-formed alveolar bone volume fraction at 4 weeks following tooth extraction (early healing). In contrast, at the ten-week evaluation period (late healing), the OVX + ALN group presented a statistically significant 2-fold higher mean bone volume fraction compared to the OVX + Pbo group (Fig. 3). Likewise, the microstructural parameters Tb.N, Conn.D and BS/TV mean values were statistically significant higher in the OVX + ALN group compared to the other experimental groups at the late healing evaluation. On the contrary, Tb.Pf and SMI displayed statistically significant lower values in the OVX + ALN compared to the other groups, whereas the parameters Tb.Th, Tb.Sp and DA mean values were comparable among experimental groups.

3.3. Newly-formed alveolar bone fractal analysis by CBCT

The fractal dimension mean values, presented in Fig. 3 C, were not different among groups at the early healing period. However, the OVX + ALN group presented a trend of lower mean values at the late healing period than the other groups ($p = 0.053$, −12% OVX + ALN vs. OVX + Pbo; −9% OVX + ALN vs. SHAM + Pbo).

3.4. Type I collagen accumulation and collagen crosslinks

Results from the spectrophotometric determination of hydroxyproline content indicated that the mean collagen result in the OVX + ALN group was twofold greater compared to the SHAM + Pbo group and was fourfold greater in relation to the OVX + Pbo group, which was similar at both healing periods (Fig. 4).

Mature, trivalent, enzyme-induced cross-links present in the newly-formed alveolar bone were calculated through the combination of DPD and PYD contents. Those cross-links were found in significant superior mean content in the OVX + Pbo group in comparison to the other two experimental groups, at both early and late healing time points (+50% OVX + Pbo vs. OVX + ALN; +25% OVX + Pbo vs. SHAM + Pbo). In Fig. 4, one can observe that the OVX + ALN group presented the least mean content of DPD + PYD, which was statistically significant in relation to the sham-operated group at both time point evaluations (−35% at 4 weeks; −26% at 10 weeks). Regarding the non-enzymatic-induced cross-link, mean results pointed to a statistically significant higher PEN mean values in the ovariectomized groups in relation to the

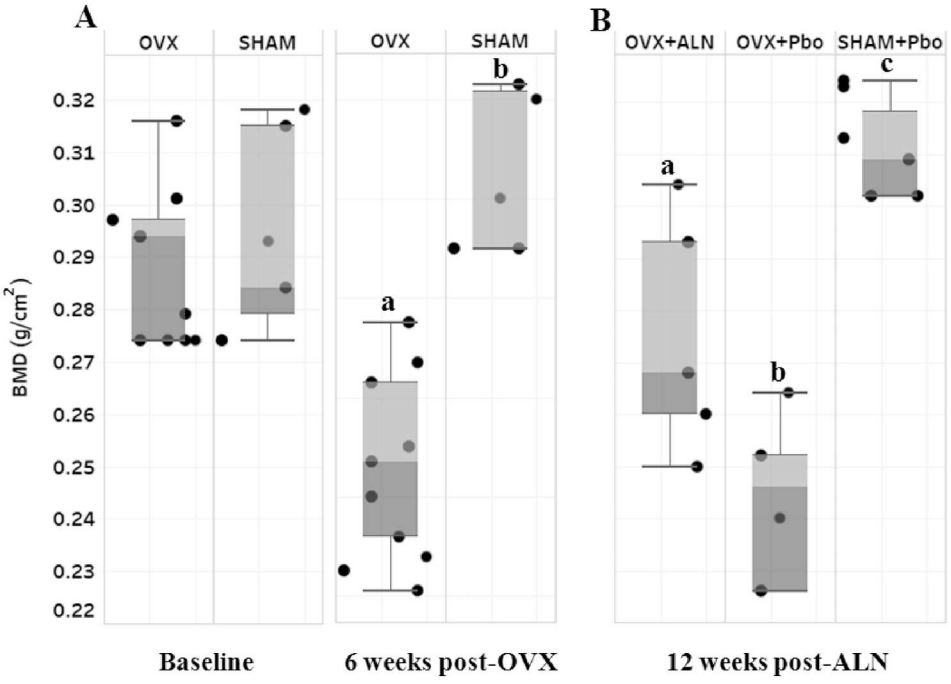

Fig. 2. Whole-body bone mineral density (BMD). A, OVX group compared to SHAM-operated group, at baseline and at 6 weeks post-surgery. B, experimental groups, OVX + ALN, OVX + Pbo and SHAM + Pbo, were compared at 12 weeks after the beginning of medication. Different letters indicate statistically significant difference within each time point ($p < 0.05$, one-way ANOVA, followed by Bonferroni *post-hoc* test).

SHAM + Pbo group (+17% OVX + ALN vs. SHAM + Pbo, +30% OVX + Pbo vs. SHAM + Pbo, at both time points). The OVX + Pbo group presented the highest PEN mean content, at both time points (Fig. 4).

4. Discussion

In the present study it was demonstrated that the antiresorptive drug ALN was capable of reversing the low BMD seen in the ovariectomized rabbits. However, ALN was not totally effective in rescuing the quality of the newly-formed alveolar osseous tissue observed in the sham-operated animals, based on a higher content of the non-enzymatic, glycation-induced, pentosidine cross-link found in the test group. Pentosidine, the most common AGE in the skeleton, has been associated with bone fragility in aged organisms or those affected by diseases, including diabetes and osteoporosis [25,26]. Fragility fractures might also be associated with the quality of type I collagen crosslinking, independently of the bone mineral density [27–29]. The clinical impact of the reduced collagen matrix quality evaluated in the healing dental alveolus may not be directly comparable to that in other skeletal sites probably due to morphological and embryological differences between them [30]. Independently of the anatomical location, an altered cross-link pattern can be used as molecular marker and might be a therapeutic target in metabolic bone disorders [31,32].

The results described here are partially validated by the whole-body DXA, which indicated that the experimental bilateral OVX combined with low calcium and phosphorus diet could reduce the BMD in rabbits in line with other authors [33]. According to one study, OVX alone would not be sufficient to induce osteoporosis in rabbits [34]. The 17% BMD reduction seen in the ovariectomized animals is lower than the 25% BMD reduction defined by the World Health Organization for the diagnosis of osteoporosis in postmenopausal women [35], what could be considered a shortcoming of the current study. A superior BMD reduction of the lumbar spine has been achieved in rabbits by supplementing the ovariectomy with daily corticosteroid injections [36]. Corticosteroid therapy in addition to ovariectomy, though, does not

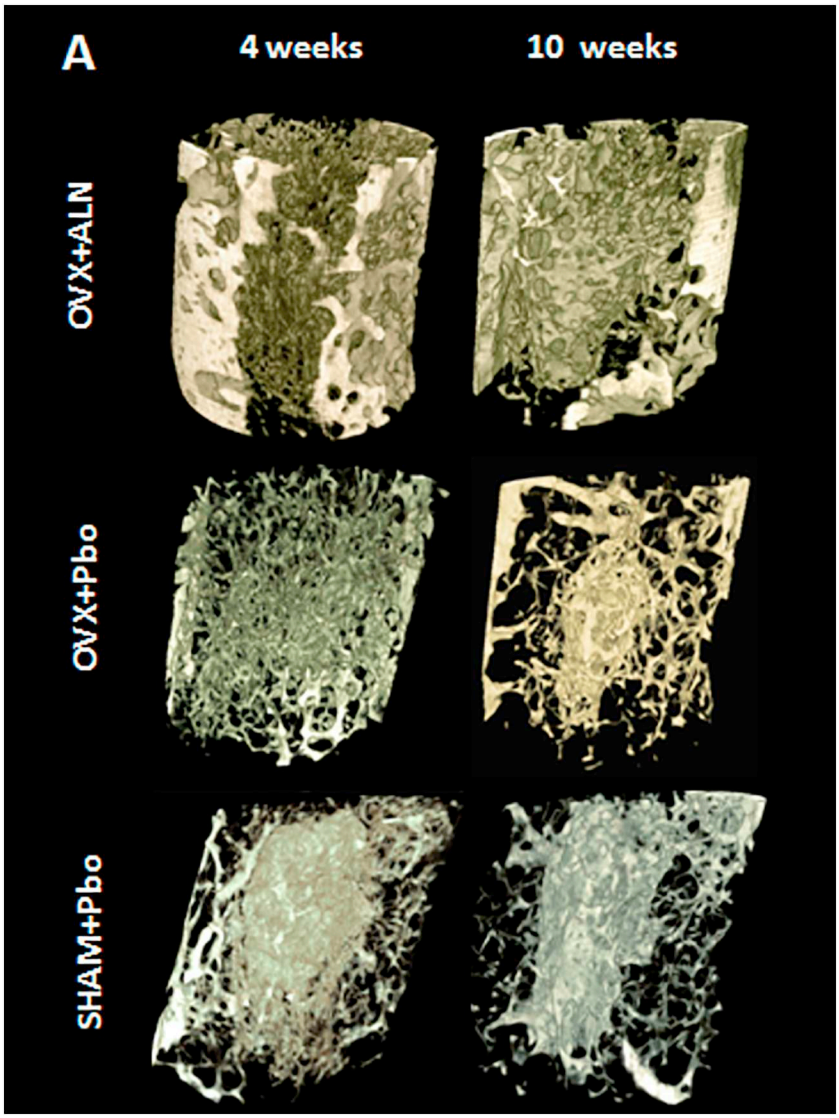

Fig. 3. Microstructural alterations in the newly-formed alveolar bone at early (4 weeks) and late (10 weeks) healing stages of each experimental group (OVX + ALN, OVX + Pbo, SHAM + Pbo). A, representative μCT reconstructed images of specimens whose mean BV/TV values at 4 weeks were closest to the respective group mean. B, morphometric comparison between experimental groups of the following parameters: bone volume fraction (BV/TV), trabecular pattern factor (Tb.Pf), structure model index (SMI), trabecular number (Tb.N), trabecular thickness (Tb.Th), trabecular separation (Tb.Sp), connectivity density (Conn.D), bone surface density (BS/TV) and degree of anisotropy (DA). C, Fractal Dimension (FD) analyzed by cone-bean computed tomography (CBCT). Different letters indicate statistically significant difference within each time point ($p < 0.05$, one-way ANOVA, followed by Bonferroni *post-hoc* test).

B

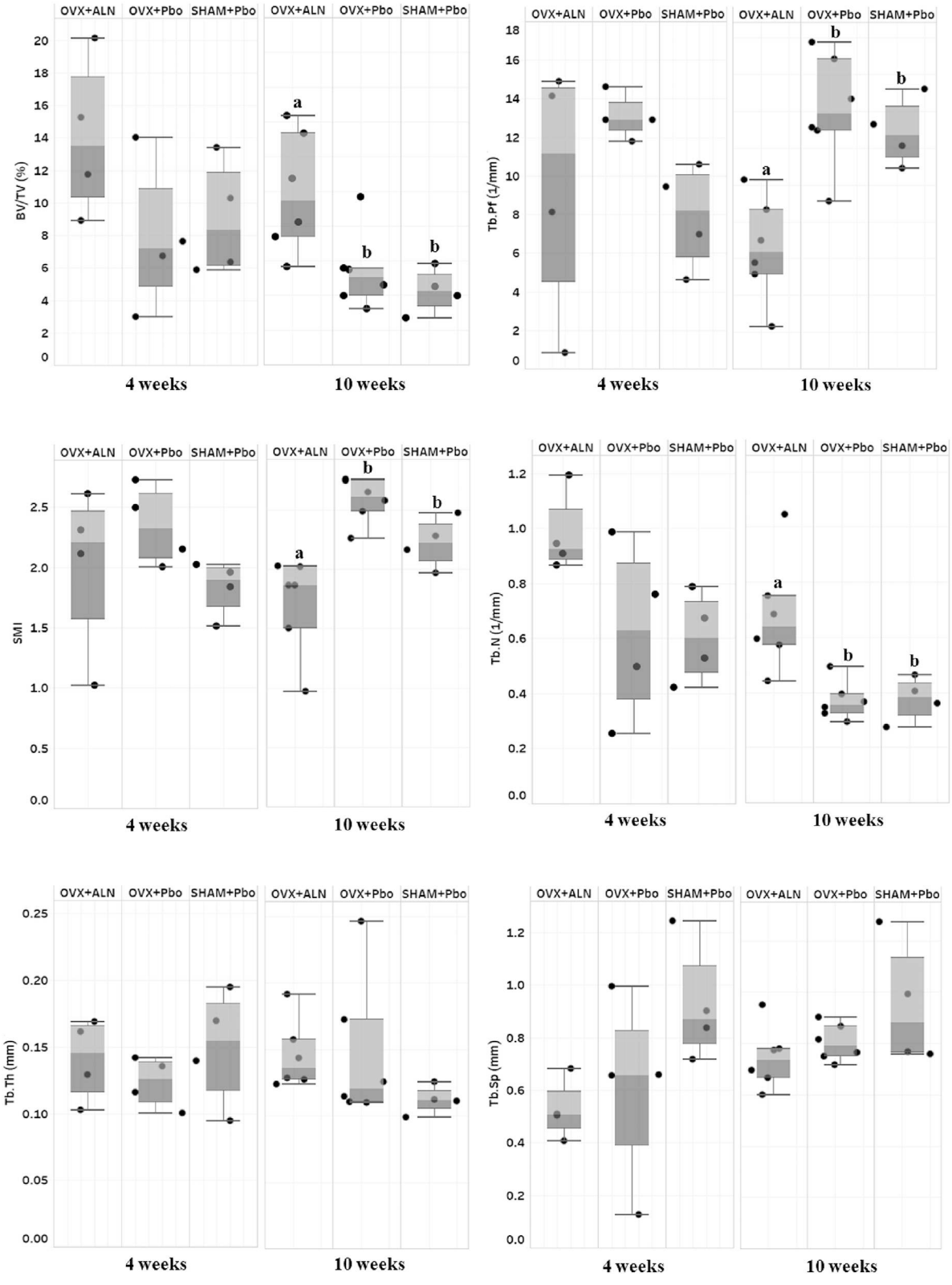

Fig. 3. (*continued*)

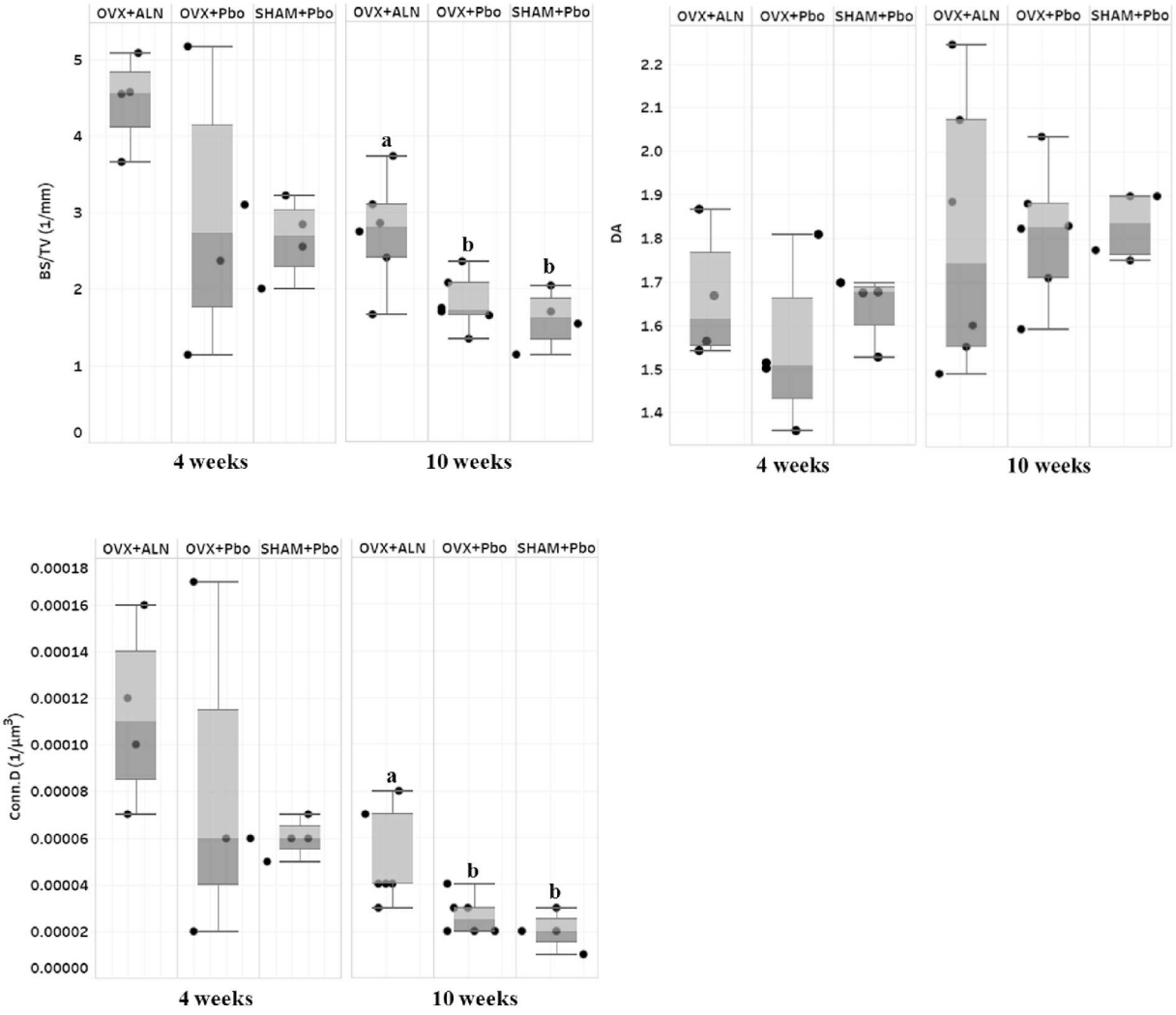

Fig. 3. (*continued*)

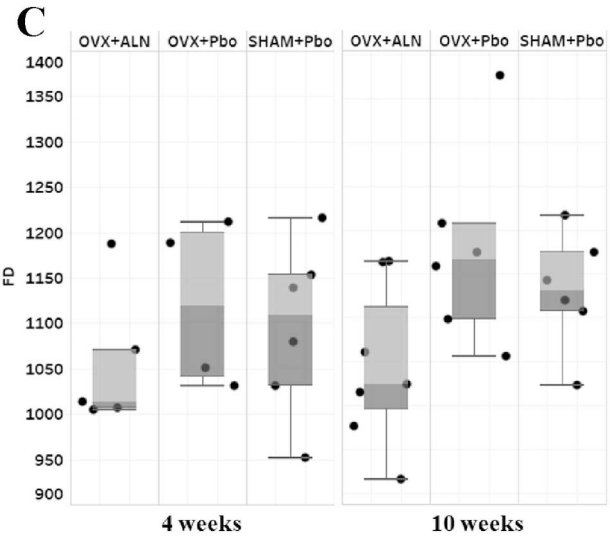

Fig. 3. (*continued*)

mimic the estrogen deficiency-induced bone loss and, in high doses, could lead to deleterious effects on tissues and even death of animals [37,38].

Rabbit is one of the most frequently employed animals in medical research, being the translational model of choice in roughly 35% of studies in the musculoskeletal field [39]. Among other advantages in relation to larger animals and even non-human primates, rabbits achieve skeletal maturity earlier and have a faster bone turnover [40]. Extrapolation of the therapeutic dose from human to animal models has important impact on the conclusion about the efficacy of the drug under investigation. An alendronate dose of 0.05 mg/kg/week given to rats by oral gavage [41], for instance, could have caused a 350-fold under exposition to the medication, whereas a dose of 2.5 mg/kg/day administered by subcutaneous via [42] might have led to a roughly 90-fold over exposed rats to the same drug. Even though, there is no universally accepted mean to calculate the equivalent dose of a certain drug, the allometric scaling based on the metabolic size and the metabolic rate is one of the commonly used methods in veterinary practice [20]. The calculation of the therapeutic dose of sodium alendronate described here and based on that established method should, therefore, be considered strength of the present investigation.

Data reported here, derived from the µCT analysis, confirm the inhibitory effect of BPs on bone remodeling since the alendronate-treated group presented a much greater bone volume fraction in comparison to the OVX + Pbo group, at the late healing phase [11]. The µCT scan, in contrast to the whole-body DXA, focused on the newly-formed osseous tissue in a specific area extending from the bottom to the mid-section of the surgical alveolus where bone repairs earlier compared with the entrance of the socket [43]. Yet, significant differences between experimental groups for most morphometric parameters presented here

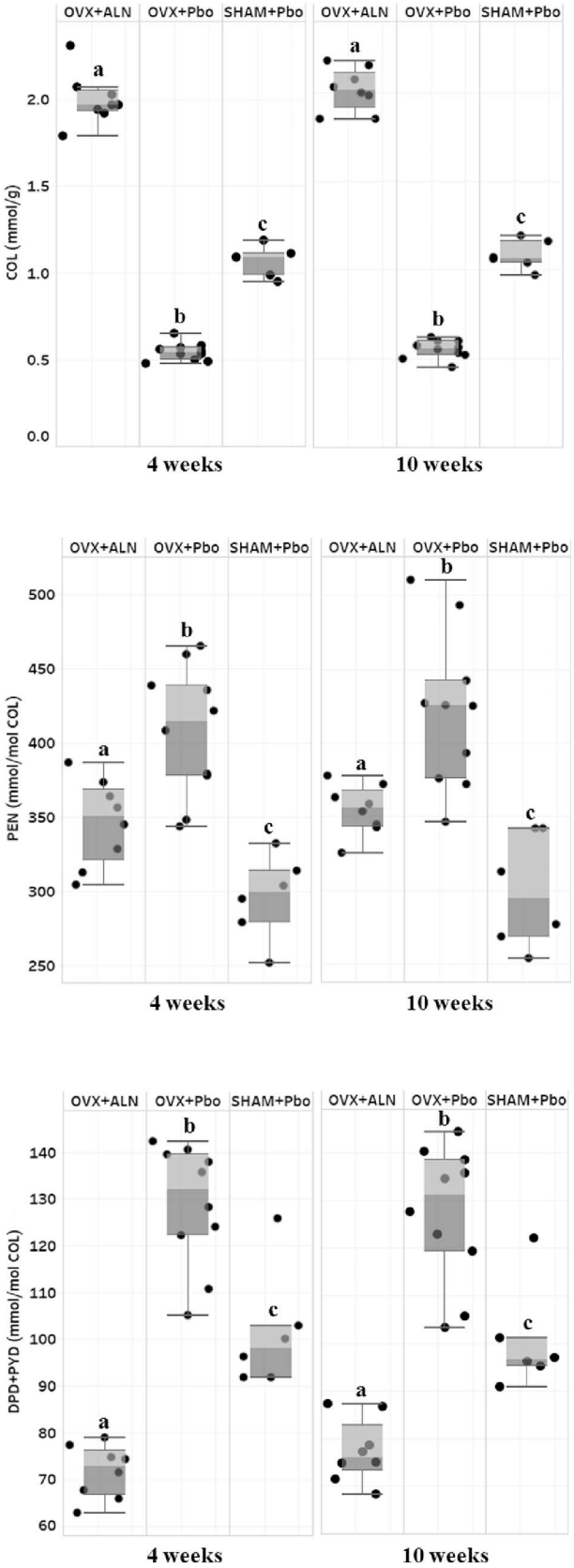

Fig. 4. Comparative spectrophotometric determination of collagen (COL) and HPLC analysis of pentosidine (PEN), and deoxypyridinoline (DPD) and pyridinoline (PYD) combined, in the newly-formed alveolar bone of the experimental groups (OVX + ALN, OVX + Pbo, SHAM + Pbo), at early (4 weeks) and late (10 weeks) healing stages. Different letters indicate statistically significant difference within each time point ($p < 0.05$, one-way ANOVA, followed by Bonferroni *post-hoc* test).

occurred at the late time point assessment, indicating a lasting healing process similar to what is observed in the dental socket of dogs [44]. For instance, the highest SMI mean result seen in the OVX + Pbo group, 10 weeks after tooth extraction, denotes a predominance of rod-like bone trabeculae due to active osteoclastic resorption. In contrast, the least SMI mean result seen in the ALN-treated group designates a plate-like trabecular pattern characteristic of a low bone turnover [45]. Other parameters including Tb.Pf, Tb.N, BS/TV and Conn.D, which reflect structure density and connectivity, are in conformity with the expected contrasting effects between high and low bone turnover. The lack of difference between experimental groups regarding the mean values of Tb.Th, Tb.Sp and DA is most likely due to the small sample size.

One should be aware that researches based on μCT scanning of dental alveoli failed to show unambiguously the effects of bisphosphonates on the bone healing process after tooth extraction [46,47]. In order to circumvent methodological issues, a redundant technique for measuring alveolar bone microarchitecture alterations such as CBCT has also been used here. Based on that instrument, the fractal analysis of the newly-formed alveolar bone pointed to a trend of increased FD values for the least bone mass as seen in the OVX + Pbo group, confirming the finding of other studies [48–50]. Conclusions in the opposite direction have been reported and could be explained by differences related to the analyzed region or to the research methodology [51,52]. Anyhow, the potential use of dental radiography as a screening test for conditions of low bone mineral density could have virtual and economic impacts on the diagnosis of postmenopausal osteoporosis [53].

A possible anabolic effect of BPs perceived in the current investigation is the highest amount of collagen accumulated in the ALN-treated group. These drugs might also stimulate osteoblast proliferation and, hence, promote the buildup of mineralized tissue [54]. The quantity of type I collagen was calculated based on its hydroxyproline (HP) content as determined by spectrophotometry. The likelihood of measuring HP-containing proteins other than collagen, manifest in the inflammatory and fibrotic phases of the socket healing, was low as animals were sacrificed and samples were collected at the earliest time point of 4 weeks after tooth extraction when the rabbit's dental alveolus is presumed to be filled mostly with lamellar bone [44,55]. Yet, our results certainly incorporate a minor amount of type III and type V collagens [25].

One of the indirect effects of BPs on decreased bone remodeling could be through the persistence of augmented pentosidine content in the collagen matrix, as demonstrated here. Since AGEs are formed between lysine residues, which are essential sites of enzymatic cross-linking in collagen molecules, their negative effects are considered to be in a competitive relationship with the positive effects of enzymatic collagen cross-links [56]. PEN is a surrogate marker of total AGE in metabolic bone diseases as it can be measured accurately in small samples by HPLC [28]. However, AGEs may not play a critical role in the regulation of bone remodeling, given that increased levels of PEN can be demonstrated in either high or low turnover bone [25,57,58]. That, in fact, corroborates the findings of the current investigation, as higher amounts of PEN were detected in both OVX + Pbo and OVX + ALN groups, respectively models of high and low bone turnover, in comparison to the sham-operated group. Yet, the highest PEN quantity seen in the OVX + Pbo group shows a relationship with increased bone resorption and may indicate poor bone strength as demonstrated in human cortical and cancellous bone [27,59]. Elevated levels of PEN in the ALN-treated group, compared to the sham-operated group, are in line with evidences of accelerated AGE cross-links formation by glyco-oxidation reactions even in newly-formed collagen and may reflect the effect of oxidative stress on the process of non-enzymatic collagen cross-linking [57,58]. This could explain a lower reabsorbing cellular activity, since there is evidence of the inhibitory action of AGEs on the process of osteoclastic differentiation, in addition to altering the structural integrity of the matrix proteins [60,61]. This change, in turn, causes increased resistance of bone to remodeling by

reducing proteolytic degradation and recycling of collagen, which favors microdamage accumulation in the mineralized tissue and its accelerated aging [62,63]. Whether those findings correlate with impaired bone material properties would depend on an extended observation period since the long-term suppression of bone remodeling by BPs in dogs caused increased mineralization, collagen maturity and excessive AGEs accumulation, resulting in a brittle bone matrix [64,65].

The highest levels of pyridinoline and deoxypyridinoline combined, as seen in the OVX + Pbo group, may indicate a reduced lysyl oxidase enzyme activity and a high spontaneous conversion of immature to mature cross-links as demonstrated in a lathyrism mouse model [66]. In contrast, the least mean amount of trivalent cross-links observed in the ALN-treated group coincides with the highest accumulation of newly-formed bone what agrees with evidences that the mineralization process itself affects cross-link maturity [67]. Even though most investigators have focused on PYD and DPD for elucidating the dynamics of enzymatic cross-linking in bone, the simultaneous assessment of both immature and mature cross-links would be the ideal experimental setup in this case [16]. Interestingly, changes in the molecular markers of collagen and collagen crosslinking happened earlier in comparison with those seen in the bone mineral density and trabecular microstructure, which were evident at the late time point evaluation. In this regard, one could argue that the structural alterations in the mineralized tissue depend on and are consequence of the molecular arrangement of the collagenous matrix [25,68].

Dental alveoli repaired with the characteristics discussed here could have diverse practical implications depending on the experimental group used as reference. Overall, the dental alveolar healing process culminates with some degree of bone resorption [43]. Preservation of alveolar bone width and height is critical for the restoration of missing teeth with root-form endosseous dental implants or other type of prosthetic device. As seen in the OVX + Pbo group, the least amount of newly-formed bone and collagen, with the highest content of pentosidine, might translate into a clinical situation of jawbone atrophy which would require bone graft ridge augmentation before prosthetic rehabilitation. In comparison, an extraction socket healed under bisphosphonate effect would likely result in better preserved dental alveolar ridge as demonstrated in a preclinical study, which might benefit the osteoporotic patient with improved osseointegration and fixation of dental implants [46]. Nevertheless, in a clinical scenario, due to the tendency of BPs to accumulate in sites of active bone formation, including a healing dental socket, the potential risk of BPs-related osteonecrosis of the jaws in osteoporotic patients undergoing oral surgery should be taken into account [12].

Studies aiming at translating the results discussed here into additional clinical benefits and at being powered adequately to allow drawing conclusions with the desirable external validity are warned [69]. In the current investigation, no sample size calculation was performed, although the majority of comparative analyzes reported here had enough power to point out statistically significant differences between groups. Moreover, *post-hoc* calculation based on the BMD (primary variable) showed adequate power for the intergroup comparisons. Nonetheless, some intergroup assessments might have endured the effect of a small sample size, which must be considered a fragility of the present study.

In summary, this experimental study confirmed the ability of ovariectomy supplemented with low levels of calcium and phosphorus diet to induce conditions of reduced mineral density in rabbits similar to that seen in osteoporosis of menopausal women. In addition, it was demonstrated that sodium alendronate was able to reverse that condition. However, the newly-formed bone presented characteristics associated with conditions found in the aged skeleton or in pathologies such as diabetes mellitus.

5. Conclusion

Sodium alendronate increases bone volume and type I collagen accumulation, but does not fully recover the quality of non-osteoporotic alveolar tissue, evidenced by the elevated amount of non-enzymatic collagen cross-link.

Conflicts of interest

None.

Acknowledgments

This study was supported, in part, by the National Council for Scientific and Technological Development (CNPq) and the Coordination for the Improvement of Higher Education Personnel (CAPES), Brasilia, DF, Brazil. The authors are indebted to Dr. Paulo Cesar Silva for his inestimable help during animal handling and surgeries and to Dr. Laura Maria Carvalho de Mendonça for helping us with the DXA exams.

Declarations of interest

None.

Author's roles

Study design: NGMC, AS, EJF-F. Study conduct: NGMC, MLFF, BCS, ACD, DPM. Data collection: NGMC, MLFF, BCS, ACD, DPM. Data analysis: DPM, EJF-F. Data interpretation: NGMC, DPM, AS, EJF-F. Drafting manuscript: EJF-F. Revising manuscript content: NGMC, DPM, MLFF, AS, EJF-F. Approving final version of manuscript: All.

References

[1] A.W. Friedman, Important determinants of bone strength: beyond bone mineral density, J. Clin. Rheumatol. 12 (2) (2006) 70–77.
[2] Y.C. Chen, W.C. Lin, Risk of long-term infection-related death in clinical osteoporotic vertebral fractures: a hospital-based analysis, PLoS One 12 (8) (2017) e0182614.
[3] J.Y. Reginster, Antifracture efficacy of currently available therapies for postmenopausal osteoporosis, Drugs 71 (1) (2011) 65–78.
[4] L.A. Beaupre, D.W. Morrish, D.A. Hanley, W.P. Maksymowych, N.R. Bell, A.G. Juby, S.R. Majumdar, Oral bisphosphonates are associated with reduced mortality after hip fracture, Osteoporos. Int. 22 (3) (2011) 983–991.
[5] A. Ghirardi, M. Di Bari, A. Zambon, L. Scotti, G. Della Vedova, F. Lapi, F. Cipriani, A.P. Caputi, A. Vaccheri, D. Gregori, R. Gesuita, A. Vestri, T. Staniscia, G. Mazzaglia, G. Corrao, BEST investigators, Effectiveness of oral bisphosphonates for primary prevention of osteoporotic fractures: evidence from the AIFA-BEST observational study, Eur. J. Clin. Pharmacol. 70 (9) (2014) 1129–1137.
[6] E.F. Eriksen, A. Díez-Pérez, S. Boonen, Update on long-term treatment with bisphosphonates for postmenopausal osteoporosis: a systematic review, Bone 58 (2014) 126–135.
[7] E. Shane, D. Burr, B. Abrahamsen, R.A. Adler, T.D. Brown, A.M. Cheung, F. Cosman, J.R. Curtis, R. Dell, D.W. Dempster, P.R. Ebeling, T.A. Einhorn, H.K. Genant, P. Geusens, K. Klaushofer, J.M. Lane, F. McKiernan, R. McKinney, A. Ng, J. Nieves, R. O'Keefe, S. Papapoulos, T.S. Howe, M.C. van der Meulen, R.S. Weinstein, M.P. Whyte, Atypical subtrochanteric and diaphyseal femoral fractures: second report of a task force of the American Society for Bone and Mineral Research, J. Bone Miner. Res. 29 (1) (2014) 1–23.
[8] P.D. Miller, E.F. McCarthy, Bisphosphonate-associated atypical sub-trochanteric femur fractures: paired bone biopsy quantitative histomorphometry before and after teriparatide administration, Semin. Arthritis Rheum. 44 (5) (2015) 477–482.
[9] A.A. Lloyd, B. Gludovatz, C. Riedel, E.A. Luengo, R. Saiyed, E. Marty, D.G. Lorich, J.M. Lane, R.O. Ritchie, B. Busse, E. Donnelly, Atypical fracture with long-term bisphosphonate therapy is associated with altered cortical composition and reduced fracture resistance, Proc. Natl. Acad. Sci. U. S. A. 114 (33) (2017) 8722–8727.
[10] X. Nogués, D. Prieto-Alhambra, R. Güerri-Fernández, N. Garcia-Giralt, J. Rodriguez-Morera, L. Cos, L. Mellibovsky, A.D. Pérez, Fracture during oral bisphosphonate therapy is associated with deteriorated bone material strength index, Bone 103 (2017) 64–69.
[11] N. Kharwadkar, B. Mayne, J.E. Lawrence, V. Khanduja, Bisphosphonates and

atypical subtrochanteric fractures of the femur, Bone Joint Res. 6 (3) (2017) 144–153.
[12] S. Cheong, S. Sun, B. Kang, O. Bezouglaia, D. Elashoff, C.E. McKenna, T.L. Aghaloo, S. Tetradis, Bisphosphonate uptake in areas of tooth extraction or periapical disease, J. Oral Maxillofac. Surg. 72 (12) (2014) 2461–2468.
[13] E. Donnelly, D.S. Meredith, J.T. Nguyen, B.P. Gladnick, B.J. Rebolledo, A.D. Shaffer, D.G. Lorich, J.M. Lane, A.L. Boskey, Reduced cortical bone compositional heterogeneity with bisphosphonate treatment in postmenopausal women with intertrochanteric and subtrochanteric fractures, J. Bone Miner. Res. 27 (3) (2012) 672–678.
[14] Z.X. Wang, A.A. Lloyd, J.C. Burket, S. Gourion-Arsiquaud, E. Donnelly, Altered distributions of bone tissue mineral and collagen properties in women with fragility fractures, Bone 84 (2016) 237–244.
[15] C. Marin, G. Papantonakis, K. Sels, G.H. van Lenthe, G. Falgayrac, R. Vangoitsenhoven, B. Van der Schueren, G. Penel, F. Luyten, K. Vandamme, G. Kerckhofs, Unraveling the compromised biomechanical performance of type 2 diabetes- and Roux-en-Y gastric bypass bone by linking mechanical-structural and physico-chemical properties, Sci. Rep. 8 (1) (2018) 5881.
[16] M. Saito, K. Marumo, Effects of collagen crosslinking on bone material properties in health and disease, Calcif. Tissue Int. 97 (3) (2015) 242–261.
[17] G.E. Sroga, L. Karim, W. Colón, D. Vashishth, Biochemical characterization of major bone-matrix proteins using nanoscale-size bone samples and proteomics methodology, Mol. Cell. Proteomics 10 (9) (2011) M110.006718.
[18] N. Mardas, F. Schwarz, A. Petrie, A.-R. Hakimi, N. Donos, The effect of SLActive surface in guided bone formation in osteoporotic-like conditions, Clin. Oral Implants Res. 22 (4) (2011) 406–415.
[19] R. Rizzoli, S.L. Greenspan, G. Bone 3rd, T.J. Schnitzer, N.B. Watts, S. Adami, A.J. Foldes, C. Roux, M.A. Levine, B. Uebelhart, A.C. Santora 2nd, A. Kaur, C.A. Peverly, J.J. Orloff, Alendronate Once-Weekly Study Group, Two-year results of once-weekly administration of alendronate 70 mg for the treatment of postmenopausal osteoporosis, J. Bone Miner. Res. 17 (11) (2002) 1988–1996.
[20] V. Sharma, J.H. McNeill, To scale or not to scale: the principles of dose extrapolation, Br. J. Pharmacol. 157 (6) (2009) 907–992.
[21] F.A. Pinheiro, C.F. Mourão, V.S. Diniz, P.C. Silva, L. Meirelles, E. Santos Junior, A. Schanaider, In-vivo bone response to titanium screw implants anodized in sodium sulfate, Acta Cir. Bras. 29 (6) (2014) 376–378.
[22] L.A. Feldkamp, S.A. Goldstein, Jesion G. ParfittAM, M. Kleerekoper, The direct examination of three-dimensional bone architecture in vitro by computed tomography, J. Bone Miner. Res. 4 (1) (1989) 3–11.
[23] S. Majumdar, R.S. Weinstein, R.R. Prasad, Application of fractal geometry techniques to the study of trabecular bone, Med. Phys. 20 (6) (1993) 1611–1619.
[24] S. Viguet-Carrin, D. Farlay, Y. Bala, F. Munoz, M.L. Bouxsein, P.D. Delmas, An in vitro model to test the contribution of advanced glycation end products to bone biomechanical properties, Bone 42 (1) (2008) 139–149.
[25] M. Saito, K. Marumo, Collagen cross-links as a determinant of bone quality: a possible explanation for bone fragility in aging, osteoporosis, and diabetes mellitus, Osteoporos. Int. 21 (2) (2010) 195–214.
[26] L. Karim, M.L. Bouxsein, Effect of type 2 diabetes-related non-enzymatic glycation on bone biomechanical properties, Bone 82 (2016) 21–27.
[27] S.Y. Tang, U. Zeenath, D. Vashishth, Effects of non-enzymatic glycation on cancellous bone fragility, Bone 40 (4) (2007) 1144–1151.
[28] S. Viguet-Carrin, E. Gineyts, C. Bertholon, P.D. Delmas, Simple and sensitive method for quantification of fluorescent enzymatic mature and senescent crosslinks of collagen in bone hydrolysate using single-column high performance liquid chromatography, J. Chromatogr. B Anal. Technol. Biomed. Life Sci. 877 (1–2) (2009) 1–7.
[29] T. Neumann, S. Lodes, B. Kästner, S. Franke, M. Kiehntopf, T. Lehmann, U.A. Müller, G. Wolf, A. Sämann, High serum pentosidine but not esRAGE is associated with prevalent fractures in type 1 diabetes independent of bone mineral density and glycaemic control, Osteoporos. Int. 25 (5) (2014) 1527–1533.
[30] A. Mavropoulos, R. Rizzoli, P. Ammann, Different responsiveness of alveolar and tibial bone to bone loss stimuli, J. Bone Miner. Res. 22 (3) (2007) 403–410.
[31] S. Yamagishi, Role of advanced glycation end products (AGEs) in osteoporosis in diabetes, Curr. Drug Targets 12 (14) (2011) 2096–2102.
[32] J.R. Furst, L.C. Bandeira, W.W. Fan, S. Agarwal, K.K. Nishiyama, D.J. McMahon, E. Dworakowski, H. Jiang, S.J. Silverberg, M.R. Rubin, Advanced glycation end products and bone material strength in type 2 diabetes, J. Clin. Endocrinol. Metab. 101 (6) (2016) 2502–2510.
[33] E. Martin-Monge, I.F. Tresguerres, L. Blanco, A. Khraisat, R. Rodríguez-Torres, J.A. Tresguerres, Validation of an osteoporotic animal model for dental implant analyses: an in vivo densitometric study in rabbits, Int. J. Oral Maxillofac. Implants 26 (4) (2011) 725–730.
[34] S. Castañeda, E. Calvo, R. Largo, R. Gonzalez-Gonzalez, C. De La Piedra, M. Diaz-Curriel, G. Herrera-Beaumont, Characterization of a new experimental model of osteoporosis in rabbits, J. Bone Miner. Metab. 26 (1) (2008) 53–59.
[35] WHO (World Health Organization), Assessment of fracture risk and its application to screening for postmenopausal osteoporosis. Report of a WHO Study Group, World Health Organ. Tech. Rep. Ser. 843 (1994) 1–129.
[36] L. Baofeng, Y. Zhi, C. Bei, M. Guolin, Y. Qingshui, L. Jian, Characterization of a rabbit osteoporosis model induced by ovariectomy and glucocorticoid, Acta Orthop. 81 (3) (2010) 396–401.
[37] M. Warman, A.L. Boskey, Effect of high levels of corticosteroids on the lipids of the long bones of the mature rabbit, Metab. Bone Dis. Relat. Res. 4 (5) (1983) 319–324.
[38] B. Grardel, B. Sutter, B. Flautre, E. Viguier, F. Lavaste, P. Hardouin, Effects of glucocorticoids on skeletal growth in rabbits evaluated by dual-photon absorptiometry, microscopic connectivity and vertebral compressive strength, Osteoporos. Int. 4 (4) (1994) 204–210.
[39] J.G. Neyt, J.A. Buckwalter, N.C. Carroll, Use of animal models in musculoskeletal research, Iowa Orthop. J. 18 (1998) 118–123.
[40] E. Newman, A.S. Turner, J.D. Wark, The potential of sheep for the study of osteopenia: current status and comparison with other animal models, Bone 16 (4) (1995) 277S–284S.
[41] M.P. Maahs, A.A. Azambuja, M.M. Campos, F.G. Salum, K. Cherubini, Association between bisphosphonates and jaw osteonecrosis: a study in Wistar rats, Head Neck 33 (2) (2011) 199–207.
[42] F.P. Yamamoto-Silva, V. Bradaschia-Correa, L.A. Lima, V.E. Arana-Chavez, Ultrastructural and immunohistochemical study of early repair of alveolar sockets after the extraction of molars from alendronate-treated rats, Microsc. Res. Tech. 76 (6) (2013) 633–640.
[43] M.G. Araújo, J. Lindhe, Dimensional ridge alterations following tooth extraction. An experimental study in the dog, J. Clin. Periodontol. 32 (2) (2005) 212–218.
[44] G. Cardaropoli, M. Araújo, J. Lindhe, Dynamics of bone tissue formation in tooth extraction sites. An experimental study in dogs, J. Clin. Periodontol. 30 (9) (2003) 809–818.
[45] M.L. Bouxsein, S.K. Boyd, B.A. Christiansen, R.E. Guldberg, K.J. Jepsen, R. Müller, Guidelines for assessment of bone microstructure in rodents using micro–computed tomography, J. Bone Miner. Res. 25 (7) (2010) 1468–1486.
[46] J.H. Jee, W. Lee, B.D. Lee, The influence of alendronate on the healing of extraction sockets of ovariectomized rats assessed by in vivo microcomputed tomography, Oral Surg. Oral Med. Oral Pathol. Oral Radiol. Endod. 110 (2) (2010) e47–e53.
[47] T. Yamazaki, N. Hiruma, Y. Miake, M. Moriguti, T. Sawada, H. Yamamoto, T. Yanagisawa, The effect of bisphosphonate on bone formation after tooth extraction in ovariectomized rats, J. Hard Tissue Biol. 22 (4) (2013) 493–500.
[48] S. Panmekiate, N. Ngonphloy, T. Charoenkarn, T. Faruangsaeng, R. Pauwels, Comparison of mandibular bone microarchitecture between micro-CT and CBCT images, Dentomaxillofac. Radiol. 44 (5) (2015) 20140322.
[49] U.E. Ruttimann, R.L. Webber, J.B. Hazelrig, Fractal dimension from radiographs of peridental alveolar bone, Oral Surg. Oral Med. Oral Pathol. 74 (1) (1992) 98–110.
[50] A.-M. Bollen, A. Taguchi, P.P. Hujoel, L.G. Hollender, Fractal dimension on dental radiographs, Dentomaxillofac. Radiol. 30 (5) (2001) 270–275.
[51] S. Ergün, A. Saraçoglu, P. Güneri, B. Ozpinar, Application of fractal analysis in hyperparathyroidism, Dentomaxillofac. Radiol. 38 (5) (2009) 281–288.
[52] I. Gumussoy, O. Miloglu, E. Cankaya, I.S. Bayrakdar, Fractal properties of the trabecular pattern of the mandible in chronic renal failure, Dentomaxillofac. Radiol. 45 (5) (2016) 20150389.
[53] R.A. Mostafa, E.A. Arnout, M.M. Abo El-Fotouh, Feasibility of cone beam computed tomography radiomorphometric analysis and fractal dimension in assessment of postmenopausal osteoporosis in correlation with dual X-ray absorptiometry, Dentomaxillofac. Radiol. 45 (7) (2016) 20160212.
[54] S. Morelli, P.S. Bilbao, S. Katz, V. Lezcano, E. Roldán, R. Boland, G. Santillan, Protein phosphatases: possible bisphosphonate binding sites mediating stimulation of osteoblast proliferation, Arch. Biochem. Biophys. 507 (2) (2011) 248–253.
[55] Y. Kuboki, F. Hashimoto, K. Ishibashi, Time-dependent changes of collagen cross-links in the socket after tooth extraction in rabbits, J. Dent. Res. 67 (6) (1988) 944–948.
[56] P.C. Trackman, Enzymatic and non-enzymatic functions of the lysyl oxidase family in bone, Matrix Biol. 52-54 (2016) 7–18.
[57] M. Saito, K. Fujii, Y. Mori, K. Marumo, Role of collagen enzymatic and glycation induced cross-links as a determinant of bone quality in spontaneously diabetic WBN/Kob rats, Osteoporos. Int. 17 (10) (2006) 1514–1523.
[58] M. Saito, K. Fujii, K. Marumo, Degree of mineralization-related collagen cross-linking in the femoral neck cancellous bone in cases of hip fracture and controls, Calcif. Tissue Int. 79 (3) (2006) 160–168.
[59] J.S. Nyman, A. Roy, J.H. Tyler, R.L. Acuna, H.J. Gayle, X. Wang, Age-related factors affecting the post yield energy dissipation of human cortical bone, J. Orthop. Res. 25 (5) (2007) 646–655.
[60] F. Gossiel, C. Hoyle, E.V. McCloskey, K.E. Naylor, J. Walsh, N. Peel, R. Eastell, The effect of bisphosphonate treatment on osteoclast precursor cells in postmenopausal osteoporosis: the TRIO study, Bone 92 (2016) 94–99.
[61] U. Valcourt, B. Merle, E. Gineyts, S. Viguet-Carrin, P.D. Delmas, P. Garnero, Non-enzymatic glycation of bone collagen modifies osteoclastic activity and differentiation, J. Biol. Chem. 282 (8) (2007) 5691–5703.
[62] C.C. Danielsen, Age-related thermal stability and susceptibility to proteolysis of rat bone collagen, Biochem. J. 272 (3) (1990) 697–701.
[63] P. Zioupos, J.D. Currey, A.J. Hamer, The role of collagen in the declining mechanical properties of aging human cortical bone, J. Biomed. Mater. Res. 45 (2) (1999) 108–116.
[64] M. Saito, S. Mori, T. Mashiba, S. Komatsubara, K. Marumo, Collagen maturity, glycation induced-pentosidine, and mineralization are increased following 3-year treatment with incadronate in dogs, Osteoporos. Int. 19 (9) (2008) 1343–1354.
[65] S.Y. Tang, M.R. Allen, R. Phipps, D.B. Burr, D. Vashishth, Changes in non-enzymatic glycation and its association with altered mechanical properties following 1-year treatment with risedronate or alendronate, Osteoporos. Int. 20 (6) (2009) 887–894.
[66] E.M. McNerny, B. Gong, M.D. Morris, D.H. Kohn, Bone fracture toughness and

strength correlate with collagen cross-link maturity in a dose-controlled lathyrism mouse model, J. Bone Miner. Res. 30 (3) (2015) 455–464.
[67] E. Durchschlag, E.P. Paschalis, R. Zoehrer, P. Roschger, P. Fratzl, R. Recker, R. Phipps, K. Klaushofer, Bone material properties in trabecular bone from human iliac crest biopsies after 3- and 5-year treatment with risedronate, J. Bone Miner. Res. 21 (10) (2006) 1581–1590.
[68] S. Pornprasertsuk, W.R. Duarte, Y. Mochida, M. Yamauchi, Overexpression of lysyl hydroxylase-2b leads to defective collagen fibrillogenesis and matrix mineralization, J. Bone Miner. Res. 20 (1) (2005) 81–87.
[69] A. Steckler, K.R. McLeroy, The importance of external validity, Am. J. Public Health 98 (1) (2008) 9–10.